



Universiteit
Leiden
The Netherlands

Control of sporulation-specific cell division in *Streptomyces coelicolor*

Noens, E.

Citation

Noens, E. (2007, September 25). *Control of sporulation-specific cell division in Streptomyces coelicolor*. Department Microbial Development (LIC) Department Electron Microscopy (LUMC/MCB), Leiden University. Retrieved from <https://hdl.handle.net/1887/12351>

Version: Corrected Publisher's Version

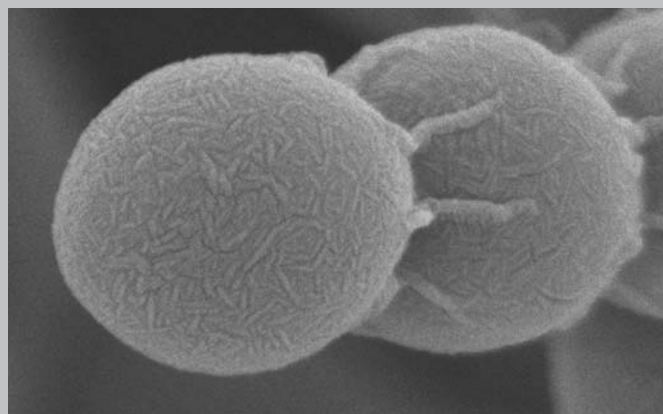
License: [Licence agreement concerning inclusion of doctoral thesis in the Institutional Repository of the University of Leiden](#)

Downloaded from: <https://hdl.handle.net/1887/12351>

Note: To cite this publication please use the final published version (if applicable).

**Analysis of cell division in the *ssg* mutants
highlights SsgB and SsgG
as important control proteins
for the initiation of septum formation**

Elke E. E. Noens, Quirinus J. M. Voorham,
Henk K. Koerten and Gilles P. van Wezel



ABSTRACT

During sporulation-specific cell division in aerial hyphae of *S. coelicolor*, a large amount of septa is simultaneously produced, in concert with the segregation and condensation of chromosomes. Members of the family of SsgA-like proteins (SALPs), exclusively occurring in sporulating actinomycetes, play a crucial role in the control of the sporulation process, from septum site selection to spore separation. The first event in sporulation-specific cell division is the localisation of FtsZ to many regularly spaced sites along the wall of the aerial hyphae. Here we show that FtsZ-rings are only infrequently produced in an *ssgB* mutant, while SsgB itself was specifically localised at sporulation septa. In an *ssgG* mutant, the typical FtsZ ladders were observed but rings were regularly missing. SsgG localised in an irregular pattern in vegetative hyphae and in two distinct patterns in aerial hyphae, but was never observed in spores. SsgG most frequently localised as well-separated foci at regular intervals, which resemble the sites for septum synthesis. Non-specific localisation of SsgE and SsgF was observed in aerial hyphae and spores. The combined deletion of *ssgA* and the suspected antagonist *ssgC* resulted in an unconditional non-sporulating, white phenotype, suggesting a functional linkage between SsgA and SsgC.

INTRODUCTION

Streptomycetes undergo two apparently different cell division events (Flårdh and van Wezel, 2003). Vegetative hyphae grow by tip extension in a DivIVA-dependent manner (Flårdh, 2003a). At this stage the hyphae are divided into multi-nucleoid compartments by vegetative septa or cross-walls. After the onset of morphological differentiation, initially aseptate aerial hyphae are erected from the lysing substrate mycelium and form a template for spore production (Chater and Losick, 1997; Chater, 2001). As development progresses, the aerial hyphae are divided into prespores by sporulation septa, which are co-synthesised to form ladders with approximately 1 μm spacing (McCormick *et al.*, 1994; Schwedock *et al.*, 1997). Control of Z-ring localisation and timing is the crucial step in the sporulation process, as this is the first step in sporulation-specific cell division (Grantcharova *et al.*, 2005; McCormick *et al.*, 1994; Schwedock *et al.*, 1997). After septum initiation, proteins responsible for the formation of the divisome are recruited sequentially to the Z-ring and septa are synthesised. At this stage, single chromosomes are segregated into the prespore compartments, the septum is closed, and the spore wall thickens. After completion of the maturation process the uninucleoid spores are separated by autolytic cleavage.

Hence, while most bacteria divide the mother cell into the daughter cells by binary fission with a single septum, up to 100 septa are produced simultaneously during sporulation of *Streptomyces*. Other important differences between cell division in sporulating actinomycetes, like *Streptomyces*, and that of other bacteria, are that cell division is not essential for growth (McCormick *et al.*, 1994; McCormick and Losick, 1996) and the apparent absence of both a *minCDE* control system for septum-site localisation (Autret and Errington, 2001; Marston *et al.*, 1998) and of Z-ring anchoring proteins such as FtsA and ZipA (Errington *et al.*, 2003f; Lowe *et al.*, 2004). This suggests that streptomycetes have species-specific proteins that play a role in the control of its complex cell division. One such family is that of the SsgA-like proteins (SALPs), a family of developmental control proteins exclusively occurring in sporulating actinomycetes (reviewed in (van Wezel and Vijgenboom, 2004)). *S. coelicolor* harbours seven SsgA-like homologues, all playing a role in certain steps of the sporulation process, from initiation of sporulation to the autolytic cleavage of mature spores (Chapter 2). The best studied example is SsgA itself, which was first identified as an effector of cell division in *Streptomyces griseus* (Kawamoto and Ensign, 1995) and specifically stimulates sporulation-specific cell division in *Streptomyces coelicolor* (van

Wezel *et al.*, 2000). Considering that FtsI is the only penicillin-binding protein (PBP) known to be part of the divisome and essential for septal peptidoglycan synthesis, we hypothesised a functional link between SsgA and the activity of FtsI (Chapter 2-4). We previously showed that in fact all SALPs are involved in specific stages of the sporulation process. SsgB is 99-100% conserved in streptomycetes and the only SALP protein present in other sporulating actinomycetes (Keijser *et al.*, 2003). Since *ssgB* mutants produce very long aseptate aerial hyphae (a strictly *whi* phenotype) it is most likely involved in a phase related to growth cessation and onset of Z-ring formation (Keijser *et al.*, 2003; Chapter 2). Similar to SsgA and SsgB, SsgG plays an important role in septum formation, and *ssgG* mutants have a distinctive light grey phenotype (indicative of less efficient sporulation). In fact, SsgG is involved in correct septum-site localisation, evidenced by the fact that during sporulation-specific cell division septa are simply 'skipped' in *ssgG* mutants, but without affecting DNA segregation (Chapter 2). Interestingly, this shows that septation is not a condition *sine qua non* for DNA segregation. The function of SsgC and SsgD is less well-defined. The similarity between *S. coelicolor* lacking *ssgC* and *S. coelicolor* over-producing SsgA (and *vice versa*) suggests that SsgC somehow antagonises the function of SsgA. SsgD is the only SALP that is abundantly produced during both vegetative and aerial growth. The thin cell wall of aerial hyphae and spores suggests that SsgD controls lateral cell wall synthesis at least during development. Finally, mutants lacking either SsgE or SsgF have well-defined spore maturation defects, and the proteins are essential for the correct timing of spore dissociation and the last steps of autolysis, respectively.

In this chapter, we provide a further functional analysis of the SsgA-like proteins, studying the effects of deletion of either of the *ssg* genes in an *ssgA* mutant background. We also investigated the localisation of the Z-ring in all *ssg* mutants and of SsgB, SsgE, SsgF and SsgG, providing novel information on the timing of their expression and their function relative to well-known developmental checkpoint events.

MATERIALS AND METHODS

Bacterial strains and media

The bacterial strains described in this work are listed in Table 1. *E. coli* K-12 strains JM109 (Sambrook *et al.*, 1989) and ET12567 (MacNeil *et al.*, 1992) were used for routine cloning and plasmid propagation and were grown and transformed by standard procedures (Sambrook

et al., 1989). *E. coli* BW25311 (Datsenko and Wanner, 2000) was used to create and propagate the *S. coelicolor* cosmids used for the creation of the fusion of SsgG with EGFP in *S. coelicolor* M145. *E. coli* ET12567 containing pUZ8002 was used for conjugation to *S. coelicolor* (Kieser *et al.*, 2000). *E. coli* transformants were selected in L-broth containing the appropriate antibiotics. *Streptomyces coelicolor* A3(2) M145 was obtained from the John Innes Centre strain collection, and was the parent for the previously created *ssgA* (GSA3) (van Wezel *et al.*, 2000), *ssgB* (GSB1) (Keijser *et al.*, 2003), *ssgC* (GSC1), *ssgD* (GSD1), *ssgE* (GSE1), *ssgF* (GSF1) and *ssgG* (GSG1) mutants (Chapter 2).

All media and routine *Streptomyces* techniques are described in the *Streptomyces* manual (Kieser *et al.*, 2000). Soy flour mannitol (SFM) agar plates were used for making spore suspensions and for microscopical analysis and R2YE agar plates for regeneration of protoplasts and, after the addition of the appropriate antibiotic, for selecting recombinants. For standard cultivation and for plasmid isolation, YEME or TSBS (tryptone soy broth (Difco) containing 10% (w/v) sucrose) were used.

Plasmids, constructs and oligonucleotides

All plasmids and constructs are summarised in Table 2. pIJ2925 (Janssen and Bibb, 1993) is a pUC19-derived plasmid used for routine subcloning. The shuttle vectors pHJL401 (Larson and Hersherger, 1986) and pSET152 (Bierman *et al.*, 1992) were used for cloning in *Streptomyces*, which both have the pUC *ori* for high-copy number replication in *E. coli* and the SCP2* *ori* on pHJL401 (around five copies per chromosome) and the *attP* sequence, allowing integration at the attachment site of bacteriophage ϕ C31, on pSET152 for maintenance in *S. coelicolor*. pIJ487 was used for direct cloning into *S. coelicolor*, which maintains in *S. coelicolor* via the pIJ101 *ori* (50-100 copies per chromosome) (Ward *et al.*, 1986). KF41 is a pSET152-derived integrative vector expressing FtsZ-EGFP (Grantcharova *et al.*, 2005).

PCRs were done with *Pfu* polymerase (Stratagene), in the presence of 10% (v/v) DMSO, with an annealing temperature of 58°C. The oligonucleotides are listed in Table 3.

A 1048 bp fragment harbouring the putative promoter region of *ssgF* (-1048/-1 relative to the translational start codon) was amplified from *Streptomyces coelicolor* M145 genomic DNA using oligonucleotides *ssgF*pr-F and *ssgF*pr-R. This section was inserted as an *EcoRI-KpnI* fragment into pIJ2925. Subsequently, *ecfp* was amplified from pECFP (BD Biosciences Clontech) using primers CFP/YFP-F2 and CFP/YFP-R2, replacing the stop

codon of *ecfp* with a *Bam*HI site. *ecfp* was inserted as a *Kpn*I-*Bam*HI fragment behind the putative promoter region of *ssgF* in pIJ2925. A 492 bp fragment containing *ssgF* was amplified from M145 genomic DNA using oligonucleotides *ssgF*-F and *ssgF*-R, replacing the start codon with a *Bam*HI site. This fragment was inserted in frame with the *ecfp* as a *Bam*HI-*Hind*III fragment in pIJ2925, resulting in pGWS157. The complete insert of pGWS157 was digested with *Eco*RI-*Bgl*III and the resulting fragment was ligated into the *Eco*RI-*Bam*HI sites of pSET152, giving the integrative vector pGWS158. The same fragment was inserted as an *Eco*RI-*Hind*III fragment into pHJL401 and into the multi-copy vector pIJ487, generating pGWS159 and pGWS163, respectively. In this way several plasmids were created that expressed *ecfp-ssgF* fusion from the natural *ssgF* promoter.

Table 1: Bacterial strains.

Bacterial strain	Genotype	Reference
<i>S. coelicolor</i> A3(2) M145	SCP1 ⁺ SCP2 ⁻	(Kieser <i>et al.</i> , 2000)
GSA3	M145 Δ <i>ssgA</i> (::aada)	(van Wezel <i>et al.</i> , 2000)
GSB1	M145 Δ <i>ssgB</i> (::aac(3)IV)	(Keijser <i>et al.</i> , 2003)
GSC1	M145 Δ <i>ssgC</i> (::aac(3)IV)	(Noens <i>et al.</i> , 2005)
GSD1	M145 Δ <i>ssgD</i> (::aac(3)IV)	(Noens <i>et al.</i> , 2005)
GSE1	M145 Δ <i>ssgE</i> (::aac(3)IV)	(Noens <i>et al.</i> , 2005)
GSF1	M145 Δ <i>ssgF</i> (::aac(3)IV)	(Noens <i>et al.</i> , 2005)
GSG1	M145 Δ <i>ssgG</i> (::aac(3)IV)	(Noens <i>et al.</i> , 2005)
GSAB	M145 Δ <i>ssgA</i> (::aada) Δ <i>ssgB</i> (::aac(3)IV)	This chapter
GSAC	M145 Δ <i>ssgA</i> (::aada) Δ <i>ssgC</i> (::aac(3)IV)	This chapter
GSAD	M145 Δ <i>ssgA</i> (::aada) Δ <i>ssgD</i> (::aac(3)IV)	This chapter
GSAE	M145 Δ <i>ssgA</i> (::aada) Δ <i>ssgE</i> (::aac(3)IV)	This chapter
GSAF	M145 Δ <i>ssgA</i> (::aada) Δ <i>ssgF</i> (::aac(3)IV)	This chapter
GSAG	M145 Δ <i>ssgA</i> (::aada) Δ <i>ssgG</i> (::aac(3)IV)	This chapter
K202	M145 + KF41	(Grantcharova <i>et al.</i> , 2005)
GSA5	GSA3 + KF41	This chapter
GSB2	GSB1 + KF41	This chapter
GSC2	GSC1 + KF41	This chapter
GSD2	GSD1 + KF41	This chapter
GSE2	GSE1 + KF41	This chapter
GSF2	GSF1 + KF41	This chapter
GSG2	GSG1 + KF41	This chapter
GSG3	M145 <i>ssgG-egfp</i>	This chapter
J3310	M145 <i>parB-egfp</i>	(Jakimowicz <i>et al.</i> , 2005)
<i>E. coli</i> JM109	See reference	(Sambrook <i>et al.</i> , 1989)
<i>E. coli</i> ET12567	See reference	(MacNeil <i>et al.</i> , 1992)
<i>E. coli</i> BW25311	See reference	(Gust <i>et al.</i> , 2003)
<i>E. coli</i> ET 12567/pUZ8002	See reference	(Gust <i>et al.</i> , 2003)

To obtain a translational fusion of *SsgE* with ECFP, a 1111 bp fragment was amplified from M145 genomic DNA using primers *ssgE*-F and *ssgE*-R, harbouring *ssgE* and 790 bp of the upstream region. The stop codon of *ssgE* was replaced with a *Kpn*I site. This section was inserted as an *Eco*RI-*Kpn*I fragment into pIJ2925. Subsequently, *ecfp* was amplified from pECFP (BD Biosciences-Clontech) with CFP/YFP-F and CFP/YFP-R, replacing the start codon with a *Kpn*I site, and inserted as a *Kpn*I-*Hind*III fragment behind *ssgE* in pIJ2925, so as

to create pGWS160 that contained an in frame fusion of *ssgE* and *ecfp*. *ssgE-ecfp* of pGWS160 was then inserted as an *EcoRI-Bg/III* fragment into an *EcoRI/BamHI*-digested pSET152, giving pGWS161 and as an *EcoRI-HindIII* fragment into the low-copy shuttle vector pHLJ401 or in the multi-copy vector pIJ487, generating pGWS162 and pGWS164, respectively. Thus, an in frame *ssgE-ecfp* fusion was created, expressed from the natural promoter of *ssgE*.

Table 2: Plasmids and constructs.

Plasmid/ Cosmid	Description	Reference
pHJL401	<i>Streptomyces/E. coli</i> shuttle vector (5-10 and around 100 copies per genome, respectively)	(Larson and Hershberger, 1986)
pIJ2925	Derivative of pUC19 (high copy number) with <i>Bg/III</i> sites flanking its multiple cloning site	(Janssen and Bibb, 1993)
pSET152	<i>Streptomyces/ E. coli</i> shuttle vector (integrative in <i>Streptomyces</i> , high copy number in <i>E. coli</i>)	(Bierman <i>et al.</i> , 1992)
pIJ487	Derivative of pIJ101 <i>Streptomyces</i> high copy vector (up to 300 copies per chromosome)	(Ward <i>et al.</i> , 1986)
pGWS157	pIJ2925 with 2.3 kb fragment harbouring upstream region of <i>ssgF</i> (-1048/-1) <i>ecfp</i> (+1/+716) and <i>ssgF</i> (+3/+495, relative to <i>ssgF</i>)	This chapter
pGWS158	pSET152 with 2.3 kb fragment harbouring upstream region of <i>ssgF</i> (-1048/-1) <i>ecfp</i> (+1/+716) and <i>ssgF</i> (+3/+495, relative to <i>ssgF</i>)	This chapter
PGWS159	pHJL401 with 2.3 kb fragment harbouring upstream region of <i>ssgF</i> (-1048/-1) <i>ecfp</i> (+1/+716) and <i>ssgF</i> (+3/+495, relative to <i>ssgF</i>)	This chapter
pGWS160	pIJ2925 with 1.9 kb fragment harbouring <i>ssgE</i> (-740/+378, relative to <i>ssgE</i>) and <i>ecfp</i> (+3/+719)	This chapter
pGWS161	pSET152 with 1.9 kb fragment harbouring <i>ssgE</i> (-740/+378, relative to <i>ssgE</i>) and <i>ecfp</i> (+3/+719)	This chapter
pGWS162	pHJL401 with 1.9 kb fragment harbouring <i>ssgE</i> (-740/+378, relative to <i>ssgE</i>) and <i>ecfp</i> (+3/+719)	This chapter
pGWS163	pIJ487 with 2.3 kb fragment harbouring upstream region of <i>ssgF</i> (-1048/-1) <i>ecfp</i> (+1/+716) and <i>ssgF</i> (+3/+495, relative to <i>ssgF</i>)	This chapter
pGWS164	pIJ487 with 1.9 kb fragment harbouring <i>ssgE</i> (-740/+378, relative to <i>ssgE</i>) and <i>ecfp</i> (+3/+719)	This chapter
KF41	pSET152-derived integrative vector expressing FtsZ-EGFP	(Grantcharova <i>et al.</i> , 2005)

For the creation of an *ssgG-egfp* fusion, the Redirect method was used as described earlier (Gust *et al.*, 2003). For this, primer pairs *ssgGred-F* and *ssgGred-R* were designed to amplify an *egfp-aac3(IV)-oriT* cassette from genomic DNA isolated from J3310 (Jakimowicz *et al.*, 2005) including a 10 amino acid flexible, glycine- and proline-rich linker to maximise the likelihood of a functional fusion protein. On either side of the cassette, 40bp extensions were added that are identical to the regions immediately upstream and downstream of the stop codon of *ssgG*. This fragment was introduced into *E. coli* BW25311, containing the cosmid E19A (with *ssgG*) as well as pIJ790 allowing extremely efficient recombination. The subsequent steps were described previously (Noens *et al.*, 2005). As a result, an in frame

fusion of *ssgG* with *egfp* was created in the genome of *S. coelicolor* M145 with an *aacC4* resistance cassette as a selectable marker. The correct insertion was confirmed with PCR and sequencing (not shown).

Table 3: Oligonucleotides.

Primer	DNA sequence	Location 5'end	Relative to
CFP/YFP-F	gactgg tacc gtgagcaagggcgaggagctgttc	+3	<i>cfp/yfp</i>
CFP/YFP-R	gct gaagc ttt tactgtacagctcctccatgccgag	+719	<i>cfp/yfp</i>
CFP/YFP-F2	gactgg tacc atggtgagcaagggcgaggagctg	+1	<i>cfp/yfp</i>
CFP/YFP-R2	gactgg tacc ctgtacagctcctccatgccgag	+471	<i>cfp/yfp</i>
ssgF-F	gct ggaatt ctcgaaatgatgatcgtcggccgca	+3	<i>ssgF</i>
ssgF-R	gactgg tacc gacggccattcctccagttgagc	+494	<i>ssgF</i>
ssgFpr-F	gactgg tacc agtggtgaccaccacgggtgtgcag	-1048	<i>ssgF</i>
ssgFpr-R	gct gaagc ttt catctccggtcacgtgtcccgtgg	-1	<i>ssgF</i>
ssgE-F	cat ggaatt cagcaggtgcacgccgatcatc	-790	<i>ssgE</i>
ssgE-R	gct gggtacc gtggccaccggctgcggctgcggc	+378	<i>ssgE</i>
ssgGred-F	gctcgggatcgcacgacgggctgcccagctcgcaggctgccggcccgagctg	+376	<i>ssgG</i>
ssgGred-R	ctcaaccgggcaagctctctgaccgctccgctcctcacatatgctggctggagctgcttc	+436	<i>ssgG</i>

Restriction sites used for cloning are presented in bold face.

Construction of the *ssgA*-*ssgX* double mutants

To obtain double mutants of *ssgA* in combination with a deletion of either of the other *ssg* genes, protoplast fusions were performed between the *ssgA* mutant GSA3 (resistant to spectinomycin and streptomycin) and either GSB1 (Δ *ssgB*), GSC1 (Δ *ssgC*), GSD1 (Δ *ssgD*), GSE1 (Δ *ssgE*), GSF1 (Δ *ssgF*) or GSG1 (Δ *ssgG*) (all resistant to apramycin) as described elsewhere (Kieser *et al.*, 2000). Protoplasts of GSA3 were mixed with a 50-fold excess of protoplasts of GSB1, GSC1, GSD1, GSE1, GSF1 or GSG1. First, Spc^RStr^R was used for the selection of GSA3. Subsequently, the desired double recombinants were selected by growth on apramycin. The double mutants were designated GSAB (Δ *ssgA*- Δ *ssgB*), GSAC (Δ *ssgA*- Δ *ssgC*), GSAD (Δ *ssgA*- Δ *ssgD*), GSAE (Δ *ssgA*- Δ *ssgE*), GSAF (Δ *ssgA*- Δ *ssgF*) and GSAG (Δ *ssgA*- Δ *ssgG*).

Protein isolation and Western hybridisation

For preparation of protein extracts, *S. coelicolor* M145 was grown on cellophane disks on SFM agar and mycelium was harvested at time points corresponding to vegetative growth (veg), aerial growth (aer) and sporulation (spo), as described earlier (van Wezel *et al.*, 2000). After subjecting the samples to SDS-gel electrophoresis, the gels were blotted onto Hybond-C

super nylon membranes (Amersham), and subsequently immunostained with antibodies directed against SsgE. Anti-SsgE antibodies were used in a 1:5000 dilution.

Microscopy

Confocal fluorescence microscopy

For fluorescence microscopy of strains expressing cell division proteins translationally fused with EGFP or ECFP, sterile coverslips were inserted at a 45° angle into SFM plates and spores were inoculated in the acute angle. After 2 days (for FtsZ-EGFP) and 5 days (for SsgE-EGFP, SsgF-CFP) and 1 to 4 days (for SsgG-EGFP) of incubation at 30°C, coverslips were removed and samples positioned in a drop of 1% agarose or water on a microscope slide. Immuno-fluorescence microscopy of SsgB was carried out as described previously (Schwedock *et al.*, 1997). For this, *S. coelicolor* M145 was grown on SFM for 3 days. Antibodies against SsgB were used in a 1:1000 dilution.

Electron microscopy

Morphological studies of surface-grown aerial hyphae and spores of *S. coelicolor* M145 and mutant derivatives by cryo-scanning electron microscopy (cryo-SEM) was performed as described previously, using a JEOL JSM6700F scanning electron microscope (Keijser *et al.*, 2003). The analysis of cross-sections of hyphae and spores with transmission electron microscopy (TEM) was performed with a Philips EM410 transmission electron microscope as described previously (van Wezel *et al.*, 2000).

RESULTS

Localisation of FtsZ in *ssg* mutants

Previously, we showed that the SsgA-like proteins (SALPs) are involved in specific steps of the sporulation process, from septum-site selection to spore maturation (Chapter 2). The first step in septation is the polymerisation of FtsZ into a Z-ring at the position where the septum will be synthesised. To verify if any of the SALPs affects Z-ring formation or if they are functional at a time prior to Z-ring formation, we expressed FtsZ-EGFP in the various SALP mutants (Fig. 1). For this, mutants were transformed with KF41, a derivative of pSET152, expressing FtsZ-EGFP from its natural promoters. We occasionally observed the fluorescence

indicative for correct FtsZ localisation in the *ssgA* mutant on mannitol-containing media (Fig. 1B), under which conditions the *ssgA* mutant is able to sporulate to some extent, while no FtsZ-EGFP foci were detected in the *ssgA* mutant on glucose-containing media. Occasionally, Z-rings were observed in aerial hyphae of an *ssgB* mutant, which fails to produce aerial septa but sporadically shows constriction in the aerial hyphae (Keijser *et al.*, 2003). The distance of the Z-rings observed in an *ssgB* mutant appeared to be similar as in a *whiH* mutant (Grantcharova *et al.*, 2005) (Fig. 1C). Vegetative cell division was not affected in *ssgB* mutants. As expected, in the light of their ability to sporulate, normal Z-ladders were produced by mutants deficient in *ssgC*, *ssgD*, *ssgE* or *ssgF* (Fig. 1D-F). Normally spaced FtsZ rings were also visualised in the *ssgG* mutant (Fig. 1H), although 15% of the rings were missing (Fig. 1I-K; arrows) or considerably less intense (Fig. 1I-J; stars) in this mutant. This may account for the lack of septa observed in an *ssgG* mutant, therefore creating prespore compartments twice as long as normal (Fig. 1G).

Creation of ECFP and EGFP fusions

To analyse the localisation of SsgG and of the spore maturation proteins SsgE and SsgF, constructs were made allowing the in frame fusion with *egfp* or *ecfp* (for details see Materials and Methods section). In brief, *ssgE* (preceded by 790 bp of upstream region) was fused in frame with *ecfp*, and the *ssgE-ecfp* fusion was inserted into pSET152, pHJL401 and pIJ487, creating pGWS161, pGWS162 and pGWS164, respectively. Since SsgF is predicted to have a single transmembrane helix, oriented with its N-terminus located in the cytoplasm (Chapter 2), we created an N-terminal fusion between *ssgF* and *ecfp*, expressed from the putative *ssgF* promoter region. Like for *ssgE-ecfp*, the *ecfp-ssgF* fusion gene was inserted into pSET152, pHJL401 and pIJ487 for expression in *S. coelicolor*, creating pGWS158, pGWS159 and pGWS163, respectively. Finally, an SsgG-EGFP fusion was constructed to localise SsgG in *S. coelicolor*. For this purpose, the REDIRECT method was used to express chromosomally encoded EGFP-tagged SsgG as a replacement for the wild type protein (Gust *et al.*, 2003). The resulting strain was designated GSG3.

Localisation of SsgB, SsgE, SsgF and SsgG

To visualise the subcellular localisation of SsgB in *S. coelicolor* M145, immuno-fluorescence microscopy using peptide-based anti-SsgB antibodies (G.P. van Wezel, unpublished) was

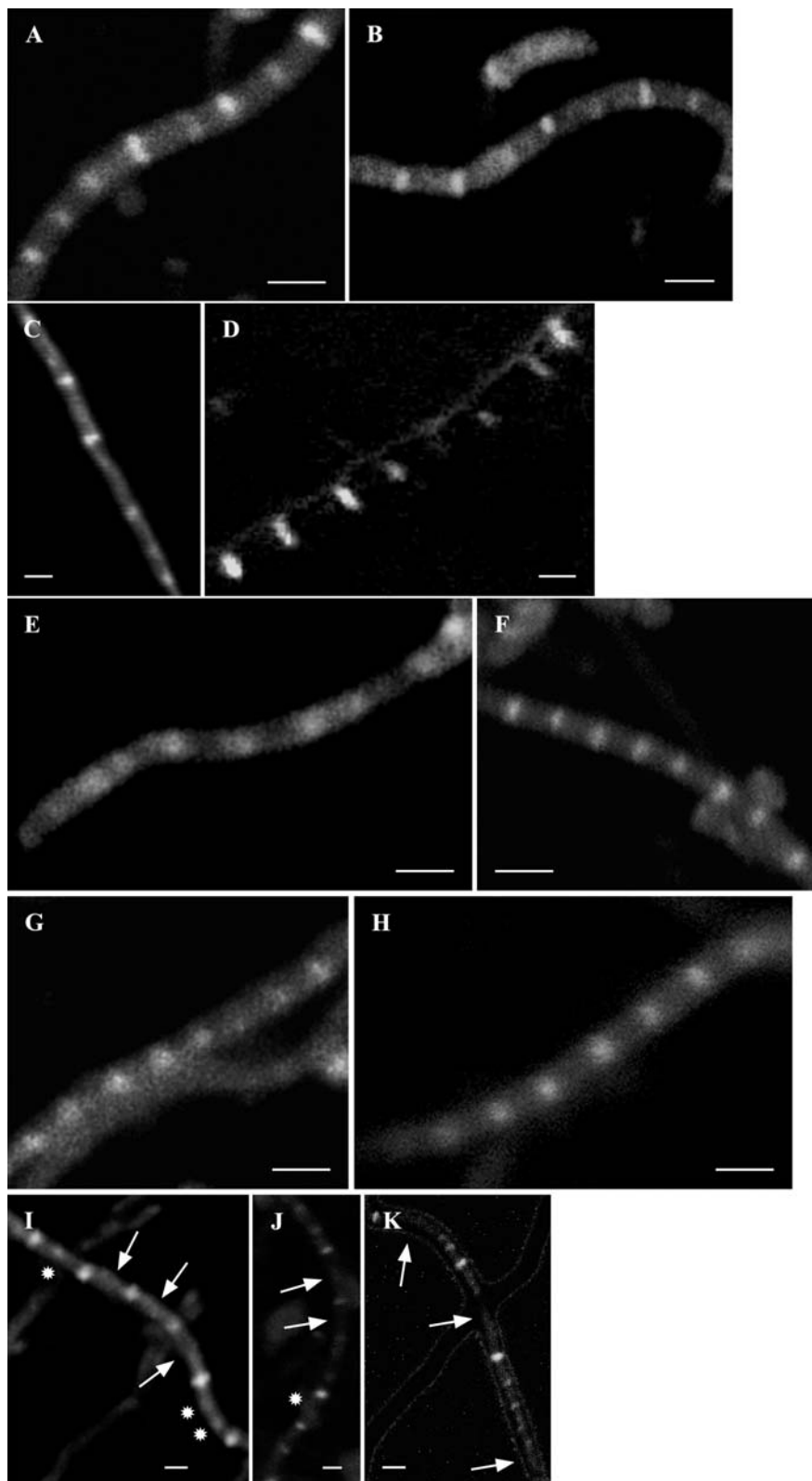
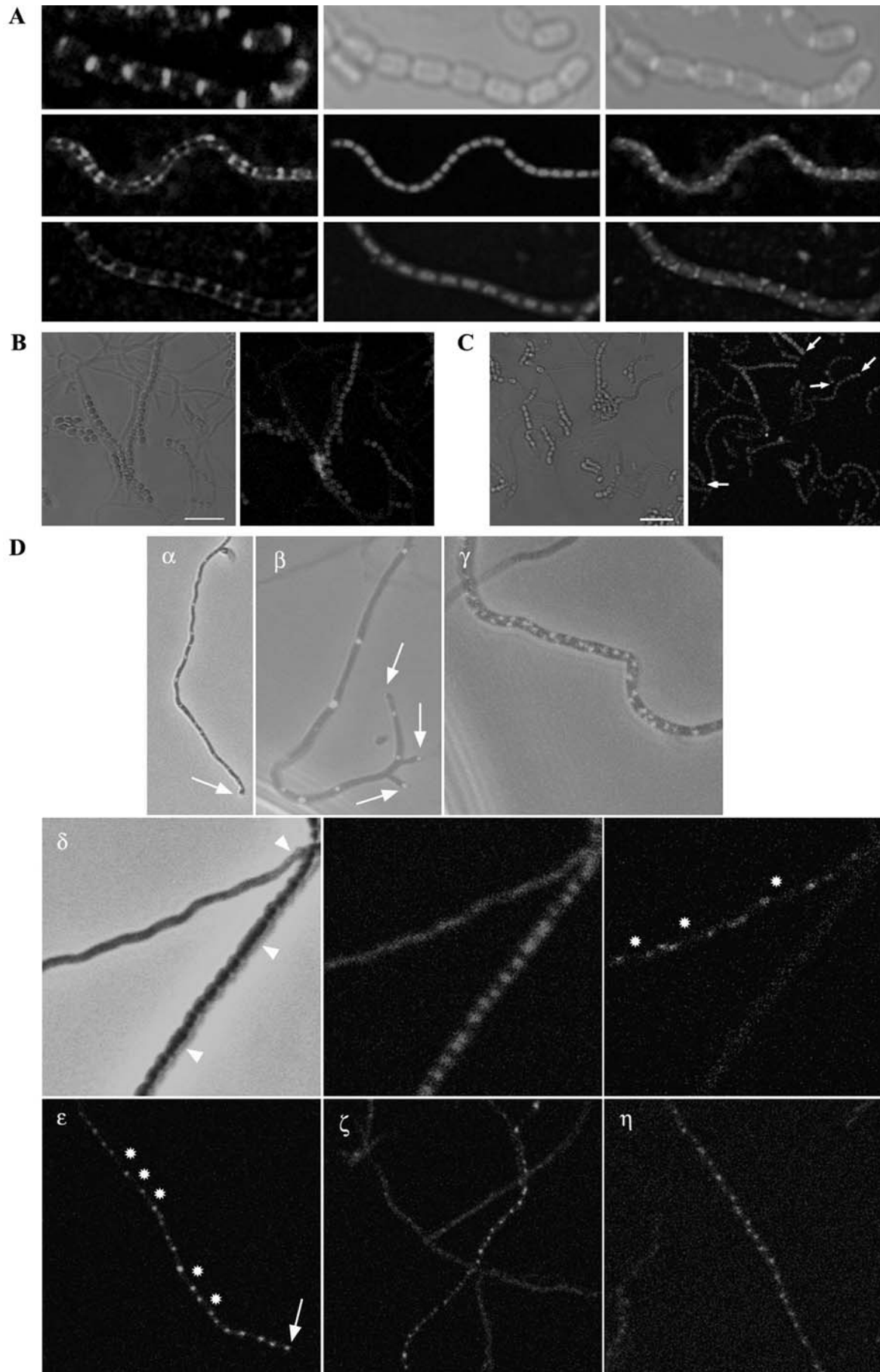


Figure 1: Localisation of FtsZ in the SALP mutants. KF41, a pSET152-derived integrative vector expressing FtsZ-EGFP, was used to localise FtsZ in *S. coelicolor* M145 (A), or its *ssgA* (B), *ssgB* (C), *ssgC* (D), *ssgD* (E), *ssgE* (F), *ssgF* (G) and *ssgG* (H-I-J-K) mutants. In the *ssgG* mutant, Z-rings are missing (arrows) or considerably less intense (stars). Strains were grown for 2 days on SFM at 30°C. Bar = 1 μm.

performed on mycelium harvested after 5 days of growth on SFM agar plates, and fixed in paraformaldehyde (see Materials & Methods). Cells were treated with lysozyme and DNA was stained with propidium iodide. Excitingly, SsgB was localised only at sporulation septa, often with the brightest fluorescence closer to the hyphal wall, leaving a distinct gap in the middle of the division ring (Fig. 2A, for a full colour version of Fig. 2, see p177-178). At this moment, the chromosomes were segregated into the prespore compartments. The timing of localisation suggests that SsgB is part of the divisome during sporulation-specific cell division. In a control experiment, we did not detect SsgB in the *ssgB* mutant (not shown).

No specific SsgE-ECFP foci were observed by confocal fluorescence microscopy in *S. coelicolor* M145 harbouring pGWS161 and pGWS164, or in GSE1 containing pGWS162. Rather, aerial hyphae and spores showed diffuse and non-specific fluorescence, with more intense fluorescence in the spores than in the aerial hyphae (Fig. 2B). GSE1 harbouring pGWS162 did not produce the free spores typical of *ssgE* mutants (Chapter 2). Therefore, the construct fully complemented the autolytic defect of *ssgE* mutants, suggesting that the fusion protein was functional and replaced the wild type SsgE (not shown). To further corroborate that the fusion protein was expressed we performed Western analysis on total protein extracts of M145 containing pGWS161 or pGWS164 and of *ssgE* mutant GSE1 harbouring pGWS162, using antibodies directed against a synthetic SsgE peptide (Fig. 3A). All three strains showed a band with a size corresponding to that of the SsgE-ECFP fusion product, indicating that the fusion protein was correctly expressed. Extracts of M145 showed a single band, corresponding to approximately three times the predicted molecular weight of SsgE (13,7kDa), while no such band was observed in extracts of the *ssgE* mutant GSE1 (Fig. 3A-B).

Figure 2: Localisation of SsgB, SsgE, SsgF and SsgG. Strains were grown on SFM for 5 days (SsgB, SsgE-ECFP and SsgF-ECFP) or 1-4 days (SsgG-EGFP) at 30°C. DNA was visualised with PI (red) **A.** Localisation of SsgB. The first column shows immunofluorescence micographs using fluorescein-conjugated anti-SsgB antibodies, the middle column shows light micrographs (top) and DNA (middle, bottom) and the third column shows overlay images from the left and the middle images. Bar = 2 μ m. **B-C.** Non-specific localisation of SsgE-ECFP (**B**) and ECFP-SsgF (**C**). ECFP-SsgF shows occasionally brighter foci at the tip of the spores (arrow). Bar = 5 μ m. **D.** Localisation of SsgG-EGFP in vegetative hyphae (α - β) and in aerial hyphae (γ - η). α - γ show overlays from light microscopy images and SsgG-EGFP. δ shows light microscopy (left), DNA (middle) and SsgG-EGFP (right) while ϵ , ζ , η show only SsgG-EGFP. In aerial hyphae, class 1 (γ) shows a staggered pattern while in class 2 (δ - η), foci are laid down in regular pattern, with distances resembling the size between sporulation septa. SsgG was not localised in the spores (δ). Stars show the place where the distance between the foci is double the normal distance and subsequently, spores two times the normal size are created (arrowheads). SsgG-EGFP appeared in the hyphal tips of both vegetative and aerial hyphae (arrows). Bar = 2 μ m. (Full colour version, see p177-178).



When *S. coelicolor* M145 transformants harbouring either pGWS158, pGWS159 or pGWS163 were analysed by fluorescence microscopy, low levels of ECFP-SsgF were detected in pGWS163 transformants, and not in pGWS158 or in pGWS159 transformants. No specific foci were detected for ECFP-SsgF (Fig. 2C). Rather, like for SsgE-ECFP, we observed diffuse (unfocused) fluorescence in aerial hyphae and spores. Occasionally, brighter foci were seen at the tip of the spores (see arrow Fig. 2C). While significantly fewer spores with a 90° rotation typical of the *ssgF* mutant (Chapter 2) were observed, pGWS159 failed to fully complement the phenotype of the *ssgF* mutant, suggesting that the fusion protein was only partly functional.

When *S. coelicolor* GSG3 - which expresses SsgG-EGFP - was studied by fluorescence microscopy, fluorescent foci corresponding to SsgG were observed already after one day of growth, in an irregular pattern in the vegetative hyphae, invariably with a single spot at the hyphal tips (Fig. 2D; α - β), a localisation similar to that of DivIVA (Flärdh, 2003b). In young aseptate aerial hyphae with non-segregated genomes, we observed specific foci of SsgG-EGFP with two different localisation patterns. The first pattern (Class 1) showed SsgG localised at regular intervals at either side of the aerial hyphae, in a staggered pattern (Fig. 2D; γ), while the second (Class 2) showed SsgG-EGFP as single foci at regular intervals of around 1 μ m in the middle of the hyphae (Fig. 2D; δ - ϵ - ζ - η). The class 2 localisation became more abundant as growth progressed with class 1: class 2 ratios of 40:60 after two days of growth and of 20:80 after four days of growth. Significantly more foci were detected in aerial hyphae than in vegetative hyphae, which is consistent with the strong upregulation of *ssgG* during development (Chapter 2). SsgG-EGFP foci were also found in the tips of the aerial hyphae (Fig. 2D, arrows). While the regularity of SsgG localisation was highly similar to that of Z-rings and septa, around 10% of the foci in class 2 were missing from the expected pattern, such that the distance between the foci was about two or more times the regular septal distance of around 1 μ m (Fig. 2D, stars). SsgG was not present in aerial hyphae with visible septa, suggesting that SsgG is only functional during the earliest stages of septum formation. In line with the occasional absence of SsgG-EGFP foci in GSG3, the strain also lacked around 10% of the spore septa (Fig. 2D; arrowheads), sometimes creating spores two or three times the normal size, with normal DNA segregation.

Hence, SsgG-EGFP could not completely revert the phenotype of *ssgG* mutants, which lack approximately 25% of the spore septa, resulting in a partial mutant phenotype.

Multimerisation of SsgE and SsgF

Recently obtained data showed that SsgA and SsgF are able to form homo-multimers *in vitro*, even under denaturing conditions, with up to five-membered multimers as confirmed by mass spectrometry of purified SsgF (Rob van der Heijden and G.P. van Wezel, unpublished data). Western analysis of total protein extracts of *S. coelicolor* M145 revealed a single band around 42 kDa, corresponding to a protein of approximately three times the predicted molecular mass of SsgE (13,7 kDa), while such a band was not observed in extracts of GSE1 (Fig. 3B). This suggests that also SsgE forms multimers, even under denaturing conditions. These preliminary experiments show that SALP proteins may function by multimerisation *in vivo*.

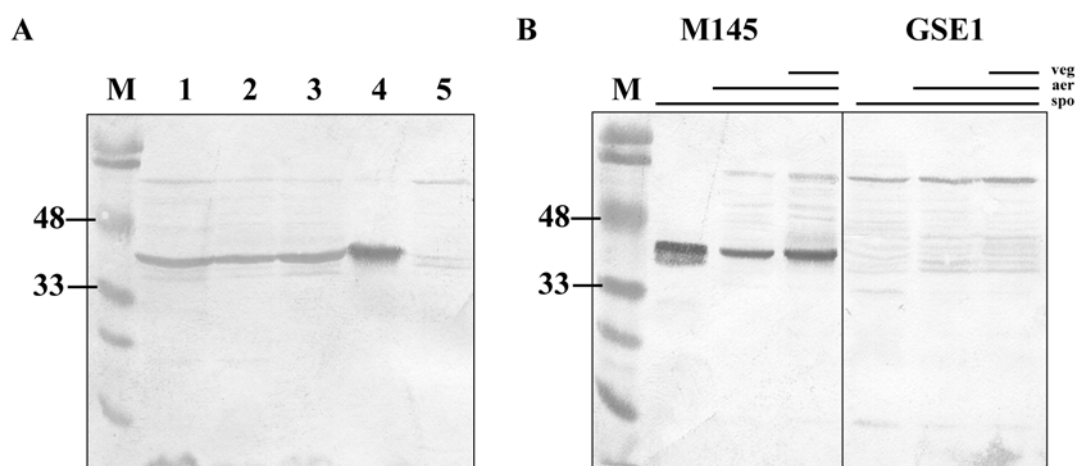


Figure 3A: Analysis of *S. coelicolor* strains expressing SsgE-ECFP. Western blot of protein extracts using antibodies against SsgE (1:5000 dilution). M: Marker; Lane 1, pGWS164 (pIJ487/*ssgE-ecfp*) in M145; Lane 2 pGWS161 (pSET152/*ssgE-ecfp*) in M145; Lane 3, pGWS162 (pHJL401/*ssgE-ecfp*) in GSE1; Lane 4, M145; Lane 5, *ssgE* mutant GSE1. The band around 42 kDa in lane 1, 2, 3 corresponds to SsgE-ECFP. The band around 42 kDa in Lane 4 corresponds to a possible SsgE trimer, which is absent from *ssgE* mutants (lane 5). **3B: Expression of SsgE.** Total protein extracts were prepared from samples of *S. coelicolor* M145 and GSE1, at time points corresponding to vegetative growth (veg), aerial growth (aer) and sporulation (spo). The band, appearing in all wild type samples, corresponding to a molecular weight of around 42 kDa is likely an SsgE trimer. This band is absent in all samples of GSE1.

Construction of double mutants

The *ssgA* mutant is able to produce spores on mannitol-containing media. Z-ring formation appeared to be normal in these sporogenic hyphae (Chapter 4) and the produced spores perform similarly as wild type spores. To investigate the effects of deletion of the other *ssg* genes in an *ssgA* mutant background and, therefore, to consider a possible redundancy between SsgA and one of the other SALPs, double mutants of *ssgA*, in combination with either *ssgB*, *ssgC*, *ssgD*, *ssgE*, *ssgF* or *ssgG* were created. For this, protoplast fusion was performed between $\Delta ssgA$ (Sp^RStr^R) and either $\Delta ssgB$, $\Delta ssgC$, $\Delta ssgD$, $\Delta ssgE$, $\Delta ssgF$ or

$\Delta ssgG$ (all Apra^R). Selection with the appropriate antibiotics gave the desired double mutants, designated GSAB, GSAC, GSAD, GSAE, GSAF and GSAG. The inactivation of the respective *ssg* genes in the double mutants was verified by Southern hybridisation.

ssgA-ssgX double mutants

To visualise the difference in the ability to sporulate, the double mutants GSAB, GSAC, GSAD, GSAE, GSAF and GSAG were plated out on SFM together with the previously made *ssgA* mutant and the wild type M145 (Fig. 4). The *ssgA* mutant GSA3 has a conditionally non-sporulating phenotype. Such a carbon-source dependence of development is found regularly in *bld* mutants (Nodwell and Losick, 1998) but is as far as we know unique for *whi* mutants: GSA3 fails to sporulate on glucose-containing media, but produces some spores on mannitol-containing media (van Wezel *et al.*, 2000). The *ssgB* mutant GSB1 displays a typical white, non-sporulating phenotype on all media (Keijser *et al.*, 2003). The other SALP mutants GSC1, GSD1, GSE1, GSF1 and GSG1 all produce grey-pigmented spores on all media, although the *ssgG* mutant GSG1 produces significantly fewer spores and thus has a lighter appearance on solid media (Chapter 2). Two double mutants GSAB and GSAC had a true carbon source-independent *whi* phenotype. The other double mutants GSAD, GSAE, GSAF and GSAG had a similar phenotype as the single *ssgA* mutant.

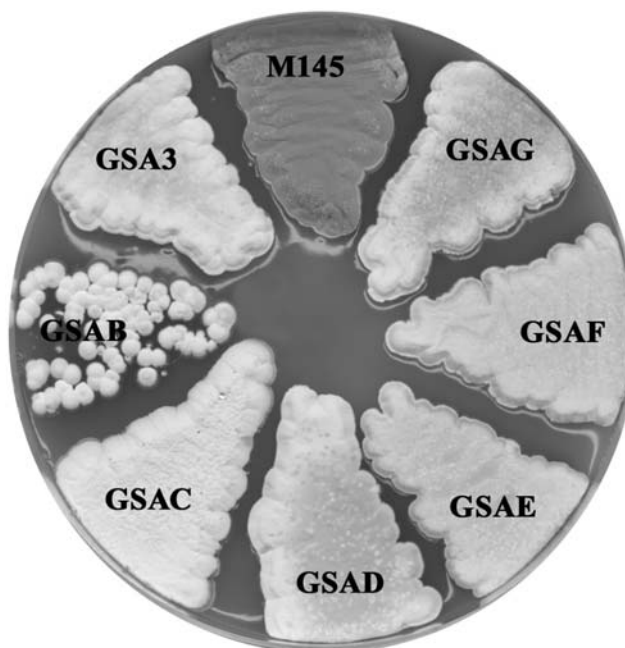


Figure 4: Phenotypes of *ssgAB*, *ssgAC*, *ssgAD*, *ssgAE*, *ssgAF* and *ssgAG* double mutants. GSAB, GSAC, GSAD, GSAE, GSAF and GSAG were grown together with M145 and GSA3 on SFM for 5 days at 30°C.

Analysis of the double mutants with electron microscopy

Surface-grown colonies of *S. coelicolor* GSAB, GSAC, GSAD, GSAE, GSAF and GSAG were analysed in detail by cryo-SEM together with the parental strain M145 and the *ssgA* mutant GSA3 (Fig. 5). *S. coelicolor* M145 produced long spore chains with spore septa at regular intervals. When we studied GSA3 with cryo-SEM, spore chains were occasionally seen and aerial hyphae were frequently lysed. Regularly, branching of aerial hyphae was observed, a phenomenon never observed in wild type aerial hyphae, possible due to a higher expression of *divIVA* in the *ssgA* single mutant (Chapter 4). All double mutants showed branching in aerial hyphae. Expectedly, the *ssgAB* double mutant GSAB produced no spores. Surprisingly, the combined deletion of *ssgA* and its suspected antagonist *ssgC* also resulted in a strictly *whi* phenotype on all media. Furthermore, branching was seen most frequently in this mutant (approximately 56% of the aerial hyphae), with sometimes up to five branches at one point in the aerial hyphae. The *ssgA* mutant phenotype was dominant over the less severe phenotypes of the single *ssgD*, *ssgE*, *ssgF* and *ssgG* mutants, which sporulate much more proficiently than the *ssgA* mutant. Except for the presence of spores, which were exactly twice the normal length in GSAG (Fig. 5; arrows), the phenotypes of GSAD, GSAE, GSAF and GSAG were very similar to that of the *ssgA* mutant.

Transmission electron microscopy was used to study the double mutants in more detail. For GSAB, TEM showed no additional features other than those reported with cryo-SEM. Strikingly, in contrast to *ssgC* mutants or strains overexpressing SsgA, no irregular or unfinished cross walls were observed in the vegetative hyphae of GSAC double mutants. GSAD and GSAG showed the particular phenotypes of the *ssgD* and *ssgG* mutants; spores with a cell wall similar to the lateral hyphal wall for GSAD (Fig. 5, GSAD; insert) and spores exactly twice the normal length for GSAG (Fig. 5, GSAG; insert), suggesting they function in an SsgA-independent manner. The spore maturation defects typical of the *ssgE* and *ssgF* mutants (free and rotated spores, respectively), were not seen in GSAE1 and GSAF1.

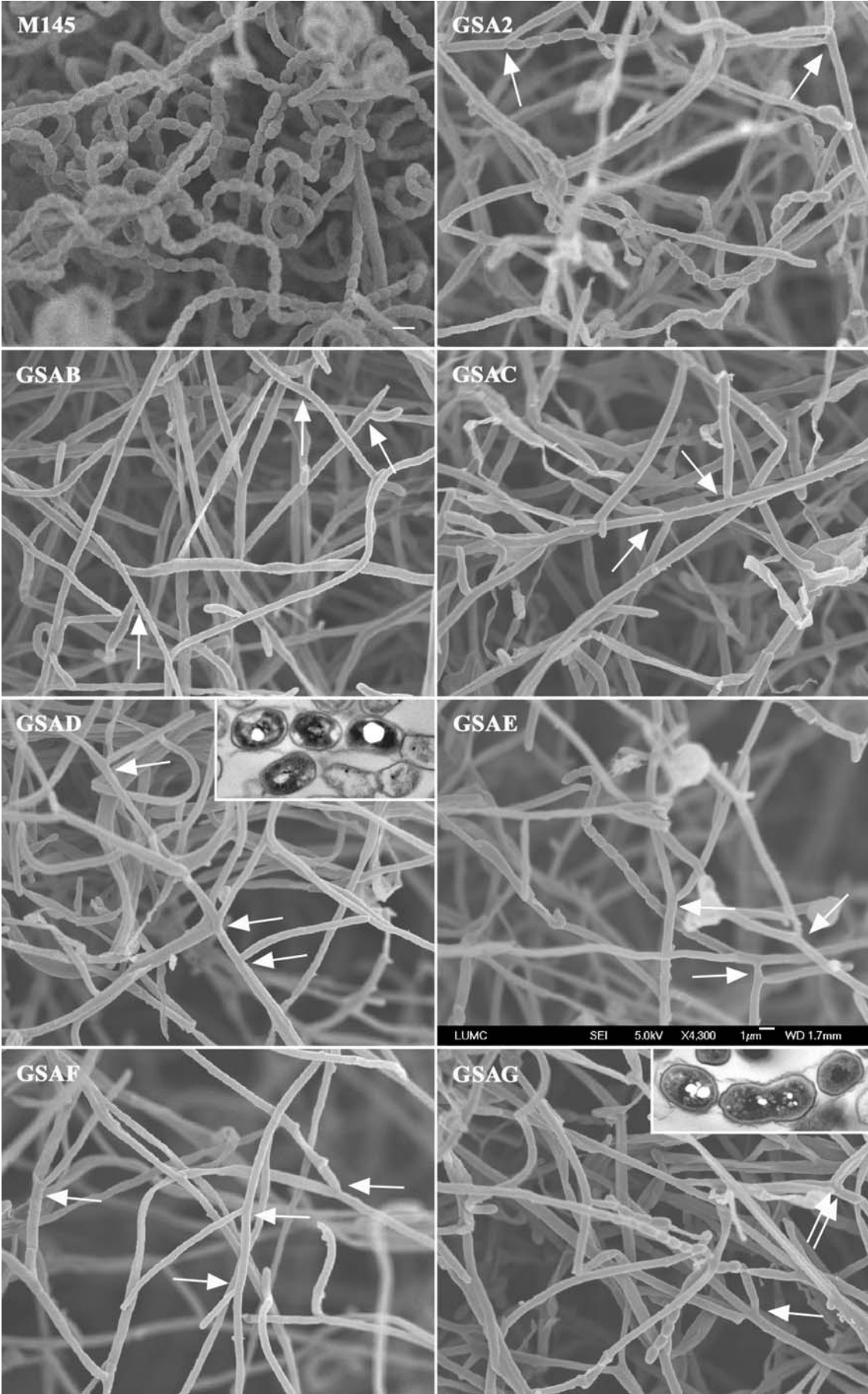


Figure 5: Cryo-scanning electron micrographs of the double mutants. Strains were grown on SFM for 5 days at 30°C. Aerial hyphae of GSA3 and all double mutants show frequently branching (arrows). Inserts of GSAD and GSAG show TEM images of typical spores for an *ssgD* and *ssgG* mutant, respectively. Bar = 1 µm.

DISCUSSION

The SALPs belong to a family of sporulation control proteins that occur exclusively in sporulating actinomycetes and are functionally linked to sporulation-specific peptidoglycan synthesis and degradation. In this chapter, we substantiate the previously published model on the function of the SALPs (Chapter 2) by dealing with three topics. These are (1) the localisation of FtsZ in sporogenic hyphae of the *ssg* mutants, (2) the localisation of SsgB, SsgE, SsgF and SsgG in hyphae and spores to provide insight into the expression of these proteins in time and space, and (3) the phenotypes of mutants with combined deletion of *ssgA* and either *ssgB*, *ssgC*, *ssgD*, *ssgE*, *ssgF* or *ssgG*, to work out if these proteins function independently of SsgA or if there is a possible functional redundancy between SsgA and one or more of the other SALPs. For example, this could perhaps explain the unique phenotype of *ssgA* mutants, which are the only conditional *whi* mutants and are able to sporulate on mannitol-containing media.

Analysis of the localisation of SsgB in *S. coelicolor* with SsgB-specific antibodies revealed specific localisation at sporulation septa in spores where DNA segregation was completed. The brightest fluorescence was mainly seen closest to the hyphal wall, with dark sections in the centre, suggesting the formation of an open ring structure. Importantly, Z-rings were only occasionally observed in aerial hyphae of *ssgB* mutants, suggesting that SsgB aids in the initial steps of Z-ring formation, and at the same time follows the growing septum. Recent data suggest that like the developmental *ftsZ* promoter (p2), transcription of *ssgB* depends on WhiH, as transcription from both promoters is almost completely absent in *whiH* mutants ((Flardh *et al.*, 2000); B. Traag and G.P. van Wezel, unpublished results). Conversely, *whiH* transcripts were detected in *ssgB* mutants. The localisation of *ssgB* itself during sporulation is in line with transcriptional analysis, showing that *ssgB* transcription is developmentally regulated, and very strongly upregulated during aerial growth, similar to the transcription of *bldN* (Chapter 2). What we know about SsgB is the following: (1) *ssgB* mutants produce normal vegetative cross walls and (2) only infrequent Z-rings in aerial

hyphae, with (3) complete failure to produce sporulation septa, (4) transcription of *ssgB* is strongly reduced in the absence of WhiH, at least in part explaining the non-sporulating phenotype of *whiH* mutants; and (5) SsgB specifically localises to the spore septa. Taken together, this strongly suggests that SsgB is part of the divisome and that the protein is essential for the growth of septal peptidoglycan, a function that is carried out by FtsI. Not unexpectedly, the additional deletion of *ssgA* had no additional effect on development, except that the double mutant had branching aerial hyphae typical of *ssgA* mutants. This suggests that SsgA and SsgB work, at least in part, independently.

Detailed phenotypic analysis suggests that SsgD is involved in correct synthesis of the lateral hyphal and spore walls and SsgE and SsgF control spore maturation (Chapter 2). As expected, the phenotype of the double mutants GSAD, GSAE and GSAF resembled that of *ssgA* mutants, which is in line with the timing of action of SsgA in the sporulation process, *i.e.* most likely prior to that of SsgD, SsgE or SsgF (Chapter 2). If SsgD, SsgE and/or SsgF function independently of SsgA, the few spores produced in the respective double mutants on mannitol-containing media should show at least some of the defects typical of *ssgD*, *ssgE* or *ssgF* single mutants. Indeed, spores of the *ssgAD* double mutant GSAD had a wall thickness similar to that of the lateral hyphal wall of aerial hyphae, a typical consequence of the deletion of *ssgD*, suggesting that SsgD functions in the absence of SsgA. In contrast, the premature spore autolysis giving rise to single spore formation in the *ssgE* mutant, or the 'rotated' spores typical of *ssgF* mutants, were not observed in the *ssgAE* or *ssgAF* double mutants. However, even though some spores were produced in the double mutants, it is almost impossible to study spore maturation defects in an *ssgA* mutant background. To learn more about the role of SsgEF in the spore maturation process and about their localisation, we studied the fate of the two proteins fused to ECFP by fluorescence microscopy. We observed non-specific localisation in the spores and aerial hyphae, with brighter fluorescence in the spores. Considering the fact that either fusion protein could restore correct spore maturation to the respective mutants, it is likely that the proteins were functional, and hence that the diffuse fluorescence truly reflects a more 'random' localisation of the protein rather than an experimental artefact such as background fluorescence. Expected, deletion of *ssgE* or *ssgF* had no effect on Z-ring formation, in line with their role in spore maturation. Further analysis is required to pinpoint the exact localisation of the two spore maturation proteins, such as immuno-electron microscopy or the use of fluorophores with stronger fluorescence.

Interestingly, the phenotype of *ssgAC* double mutants was the only one that did not simply reflect the combined defects of the single mutants, but rather displayed an almost completely non-sporulating *whi* phenotype under all conditions. Indeed, it was almost impossible to find any spores at all, and eventually no more than three spore chains could be identified with cryo-SEM. This indicates that SsgA and SsgC are functionally linked. Previously, we suggested that SsgC may have an antagonistic function towards SsgA, as the phenotype of an *ssgC* mutant is similar to that of GSA2, a strain over-expressing SsgA (Chapter 2; van Wezel *et al.*, 2000), while *vice versa*, overexpression of SsgC strongly inhibits development. Furthermore, sporulation of *ssgA* mutants can be restored by the introduction of additional copies of *ssgC* (G.P.van Wezel, unpublished results). A possible hypothesis is that SsgA and SsgC both carry out similar functions and are functionally redundant, but hetero-complexes of SsgA and SsgC are inactive. Thus SsgC negatively controls the activity of SsgA, as part of the SsgA pool is titrated out (SsgA is expressed at a higher level than SsgC in *S. coelicolor* M145). Without SsgC, more functional SsgA is available disturbing the finely tuned balance of functional and non-functional SsgA and resulting in hyperseptation of both vegetative and aerial hyphae and irregular spores. A strain with enhanced expression of SsgC would thus effectively resemble *ssgA* mutants, while in the absence of SsgA, the SsgC protein would (partly) take over its function (G.P. van Wezel, pers. comm.). Again in support of the hypothesis postulated above, in the absence of both SsgA and SsgC (in double mutant GSAC), no irregular septa were observed in vegetative hyphae. Until now, we did not succeed in localising SsgC in hyphae and spores of *S. coelicolor*, which may be due to the low expression of *ssgC* from its own promoter.

Transcriptional analysis revealed that SsgG is upregulated slightly during vegetative growth and strongly from early aerial growth (Chapter 2). This is the likely explanation why we observed foci of SsgG-EGFP in both vegetative and aerial hyphae. SsgG-EGFP was observed in aerial hyphae in two localisation patterns; class 1 with a staggered pattern and class 2 showing a ladder-like pattern. It is suggestive that the two classes of patterns observed in aerial hyphae are sequential, as the amount of class 1 decreased over time and was always observed at a lower level than class 2, indicative of its shorter lifespan. In contrast, the amount of the class 2 increased over time. This ladder-like localisation pattern strongly suggests that SsgG localises to the early septum site, corresponding to our earlier evidence that SsgG is involved in septum-site localisation (Chapter 2). The regular ‘gaps’ in the

otherwise regular distribution of SsgG-EGFP correspond very well to the frequency at which septa are lacking and result in double- or triple-sized spores, and are probably due to the fact that SsgG-EGFP fails to fully complement the *ssgG* mutant. Thus, these experiments provide further evidence that SsgG is involved in septum site selection. Excitingly, FtsZ-EGFP localisation was different in *ssgG* mutants as compared with the regularly spaced Z-rings in the wild type strain, with several 'sports' missing in the typical FtsZ ladders. Also, less intense rings were observed, probably reflecting unfinished and non-functional Z-rings. It was suggested previously that streptomycetes need a specific cell division protein for the reorganisation of the pattern of Z-ring formation from the spiral-shaped intermediate to the ladder-pattern (Grantcharova *et al.*, 2005). We suggest that SsgG is involved in this process and this may explain the localisation as a staggered pattern (class 1) as an intermediate to restructure the Z-ring into rings. SsgG is certainly not the only protein involved in the reorganisation of the Z-ring, as normal ladders are still produced in an *ssgG* mutant. In this light, it is important to note that in *ssgB* mutants only very infrequent Z-rings were observed, a phenotype similar to that of *whiH* mutants (Grantcharova *et al.*, 2005; Schwedock *et al.*, 1997). Conversely, in *ssgG* mutants septa are 'missing' around once per 5 μm . We hypothesise that SsgB and SsgG are essential for septum site localisation and have complementary functions in septum site selection, with around 80% of the septa dependent on SsgB and around 20% dependent on SsgG. Besides its function in septum-site localisation, we provide evidence that SsgB also acts as a molecular chaperone for the PBPs responsible for septal PG synthesis (FtsI and/or the developmentally controlled FtsI-like proteins SCO3156 and SCO3771; see Chapter 2). The co-localisation of *ssgB* and SsgG in the same background and the analysis of a double mutant of *ssgB* in combination with *ssgG* would help us to develop this concept further.

ACKNOWLEDGEMENTS

We thank Klas Flärth for plasmid pKF41 and for discussions.